ACS APPLIED POLYMER MATERIALS

pubs.acs.org/acsapm
Article

Design and Production of Functionalized Electrospun Fibers for Palladium Recovery

Luigi Piero Di Bonito,* Paraskevas Kyriacou, Antonio Di Colandrea, Francesco Di Natale, Giovanna Ruoppolo, and Theodora Krasia-Christoforou

Cite This: ACS Appl. Polym. Mater. 2024, 6, 9406−9419
Read Online

ABSTRACT: Adsorption stands out as a leading wastewater treatment method for ion removal or recovery. Polymeric fibers, notably electrospun ones, are gaining prominence due to their high capacity and easy recovery. Electrospinning offers a cost-effective means to produce fibers with a large surface area and high adsorption capacity. These fibers can be further functionalized with chemical substances acting as specific ligands for metal ions, bolstering their adsorption capabilities. In this study, dithioester-functionalized electrospun fibers were synthesized as an alternative to conventional sorbents for palladium recovery from acidic chloride solutions, similar to those used in hydrometallurgical processes for platinum group metal recovery (Pd, Pt, Rh···) from spent catalysts. Fibers with identical chemical composition but varying morphology were examined to assess their impact on palladium adsorption efficiency (i.e., beads-free and beads-on-string morphologies). Experimental investigations involved model solutions with varying palladium concentration, temperature, acidity (adjusted with HCl content), and salinity (adjusted with NaCl), utilizing both pure and dithioester-functionalized fibers. Experimental results demonstrate enhanced adsorption efficiency at lower temperatures and in 0.1 M HCl, with a negligible influence from solution salinity. Moreover, both pure polymeric and dithioester-functionalized electrospun fibers exhibit highly efficient palladium recovery. Furthermore, under optimal conditions, starting from an 80 mg/L palladium solution, a 95% recovery of palladium can be achieved with a sorbent dosage below 4 g/L of functionalized electrospun fibers. The adsorption data are well described by the Langmuir isotherm model for the pure polymeric fibers. At the same time, the contribution of dithioesters has been separately accounted for to describe the behavior of functionalized electrospun fibers. Thermal recovery of palladium from the spent sorbents has also been investigated.

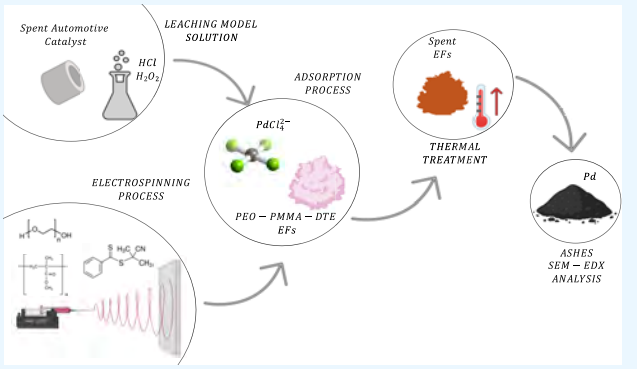

KEYWORDS: *electrospinning, polymeric fibers, palladium recovery, adsorption, dithioesters*

1. INTRODUCTION

Electrospinning is a highly versatile electrohydrodynamic process employed in the fabrication of nano- and microfibers at a laboratory and industrial scale.[1] Electrospun fibers (EFs) are successfully adopted in several fields including biomedicine, packaging,[2−5] optoelectronics, air filtration, wastewater treatment, and desalination.[6,7] Owing to their unique physicochemical properties such as high porosity, large surface areas, mechanical and chemical resistance, fibers' interconnectivity, and small diameters,[8,9] combined with their tunable chemical composition and possibility of surface functionalization,[10,11] EFs attract considerable attention as adsorbents for the removal of hazardous heavy metal ions from aqueous solutions.[12]

In nature, the existence of hazardous metal ions in water at concentration levels that can be harmful to humans and the environment is rare. On the other hand, such metal ions are present in several process waters derived from tanning, dyeing, steel manufacturing, mining activities, etc. They can also be found in natural waters that come into contact with polluted sediments or with solid waste in land disposal facilities. Restrictive regulations occurring in several countries impose treatment of such waters before their release into the environment or the remediation of polluted natural water to restore pristine environmental quality.

Adsorption is one of the most powerful methods to remove heavy metal ions that are present in water streams at

Received: January 30, 2024
Revised: April 29, 2024
Accepted: May 1, 2024
Published: August 5, 2024

concentrations ranging from a few ppb to hundreds of ppm.[13,14] Adsorption is used not only to treat wastewater or polluted natural waters but also to separate heavy metals from waters derived from industrial processes.

Ion adsorption from water streams relies on physicochemical interactions developed between the solvated metal ions and the functional groups that are present on the surface of the sorbent. To ensure appreciable adsorption, sorbent−metal ion interactions must be stronger than solvent−metal ion interactions. A useful guide to identifying the preferred functional groups is reported by Pearson and Alfarra and co-workers, and it is based on the hard soft acid base (HSAB) theory.[15,16]

The possibility of using different polymers as pristine materials for generating cost-effective adsorbents, further doping them with specific chemical moieties, and producing micro- and nanofibers characterized by high (largely accessible) surface areas renders electrospinning a valuable technique to produce highly efficient (nano)fibrous functional sorbents capable of selectively capturing metal ions from aqueous media.[17] Several literature examples exist on electrospun (nano)fibrous metal ion sorbents either in the form of pure polymeric fibers[18,19] or as functionalized analogues.[20,21]

One of the most interesting applications of EFs deals with the treatment of process water streams containing precious or rare-earth metals. For this kind of application, the fabrication of sorbents that demonstrate high adsorption capacity and selectivity toward the targeted metals is desirable owing to the high value of such metals. Consequently, higher unit costs of such sorbents can be acceptable.

Several reports available in the literature focus on the fabrication of EFs for use as adsorbents for the removal of precious metal ions from aqueous media. In one such example, we have developed magnetically functionalized fibrous adsorbents via electrospinning, consisting of random copolymers of the type poly(methyl methacrylate)-random-poly(2-(acetoacetoxy)-ethyl-methacrylate) (PMMA-*co*-PAEMA) bearing β-ketoester metal ion binding moieties, combined with poly(ethylene oxide) (PEO) and preformed oleic acid-coated magnetite nanoparticles that were successfully employed in the recovery of Eu(III).[22] In other studies of our group, pristine and magnetically functionalized polyvinylpyrrolidone (PVP)/chitosan blended nanofibers have been successfully used as sorbents for U(VI) ions,[23,24] while the introduction of magnetic nanoparticles onto the fibers' surfaces resulted in an enhancement in the adsorption capacity of the nanocomposite fibrous adsorbents compared to that of the pristine fibrous analogues, reaching 183 mg/g. Thiourea-grafted electrospun polyacrylonitrile (PAN) fibers have been used for efficient Au(III) recovery from aqueous media.[25] By combining carbonized PAN-EFs and magnetite particles, adsorption capacities of 226, 191, and 171 mg/g for Ge(IV), Ga(III), and In(III) metal ions, respectively, were achieved.[26] PAN-based EFs functionalized with natural keratin could recover up to 99% of Au(III) and 37% of Pt(IV). The higher selectivity toward Au(III) was attributed to the difference in electronegativity of the two precious metals.[27] Moreover, lignosulfonate-activated carbon EFs (LACF) were further activated with CO_2 to recover Cu(II) and Au(III) from aqueous solutions.[28]

One of the most interesting applications requiring the use of highly effective adsorbents is the hydrometallurgical treatment of spent catalysts or Waste of Electric and Electronic Equipment (WEEE), in which selective leaching processes are applied to dissolve precious metals from the waste materials.[29−31] These process waters are often acidic (thus promoting oxidation) and contain strong oxidants that transform the elemental (insoluble) metallic nanoparticles (e.g., Pd(0) and Au(0)) that are present on the waste material into solvated metal ions (e.g., Pd(II) and Au(III) ions).[32−34] Ligands are also present to promote metal ion solvation in the acidic environment (e.g., forming $PdCl_4^{-2}$ and $Au(CN)^{2-}$), favoring metal dissolution. Chlorides, cyanides, and thiols are widely used as ligands for platinum group metals, gold, copper, nickel, etc., while oxidants include among others nitric acid, hydrogen peroxides, and hydrofluoric acid.[35−38]

One typical example of such a process involves the use of diluted aqua regia.[39] In these solutions, the ions must be recovered after the solid waste is removed at the end of the leaching step.[40] At this stage, adsorption can be employed as a valid option in refining the process water to recover the metals and, possibly, in restoring the pristine leaching solution.[41]

Herein, we describe the development of functionalized EFs that can be potentially used in the recovery of precious metals (particularly palladium) from spent catalysts and WEEE, in line with the development of sustainable hydrometallurgical processes. To this end, model aqueous solutions containing palladium were prepared, resembling those derived from hydrometallurgical treatments of spent catalysts. The prepared solutions were based on leaching with hydrogen peroxides and hydrochloric acid/chloride salts, and they were similar to those adopted in a former publication of our group dealing with platinum recovery.[42]

According to previous literature findings, activated carbons can be used in the associated refining process, exhibiting adsorption capacities in a range of 5−50 mg/g.[43,44] 2-Thionicotinic acid-modified PAN EFs were used as adsorbents for Pd(II) from spent catalyst leaching solutions, achieving a maximum uptake capacity of 348.4 mg/g.[45] In such solutions, palladium ions are mostly found in the form of $PdCl_4^{-2}$ anions, which are electrostatically attracted by positively charged sorbents. The Pd(II) ions are soft acids[15,16] that interact preferentially with R-SH_x and R-NH_x rather than with R-OH_x surface functional groups. Therefore, the sorbent material should have a pH_{PZC} higher than the solution pH and should incorporate R-SH_x or R-NH_x groups to favor the conversion of $PdCl_4^{-2}$ anions into Pd−S or Pd−N bonded surface sites. The sorbent can also benefit from the presence of C=C bonds, which can react with Pd(II). In addition, the sorbent must be stable in an acidic environment, while it is not necessary to have a high thermal stability since adsorption is commonly preferred at lower temperatures and treatment of acid−water mixtures at temperatures above 60 °C is unreliable due to the evaporation of acid gases.

To this end, we designed a new sorbent based on poly(ethylene oxide) (PEO) and poly(methyl-methacrylate) (PMMA) doped with different amounts of a dithioester, namely, 2-cyano-2-propyl benzodithioate (DTE). The sorbent has been produced in the form of electrospun fibers and tested in the model aqueous solutions, as a function of pH, salinity, and temperature. Different characterization methods were used for obtaining information on the morphological characteristics and Pd(II) adsorption efficiency of the produced EF sorbents, as a function of various physicochemical parameters. Moreover, comparative studies were carried out using EFs having the same chemical composition but different morphology (i.e.,

https://doi.org/10.1021/acsapm.4c00324
ACS Appl. Polym. Mater. 2024, 6, 9406−9419

beads-free and beads-on-string) as Pd(II) sorbents. The beads-on-string morphology derives from an undesired effect of jet instability during electrospinning, which gives rise to a more or less regular sequence of beads connected with tiny fibers. In most studies, electrospun fibers characterized by a beads-on-string morphology are discarded and optimization of the electrospinning processing parameters is carried out to obtain beads-free fibers. Only recently, it has been demonstrated that beads-on-string fibers may present an equal or even better performance in comparison to their beads-free counterparts, and consequently, they could be used in biomedical applications, water and air filtration, thermal energy storage, etc.[46−48] Experimental tests have been carried out in batch mode, and experimental results have been interpreted by using a standard theory for heavy metal adsorption. The properties of spent sorbents have been investigated, and a preliminary assessment of the thermal recovery of the adsorbed palladium has also been exhibited.

2. MATERIALS AND METHODS

2.1. Electrospun Fiber Production. Poly(ethylene oxide) (PEO, average molar mass 600,000 g/mol), poly(methyl methacrylate) (PMMA, average molar mass 350,000 g/mol), and the dithioester 2-cyano-2-propyl benzodithioate (DTE, grade >97%, HPLC grade) were obtained from Sigma-Aldrich Chemie GmbH, (Tauflirchen, Germany). Chloroform ($CHCl_3$, ACS reagent grade) was purchased from Scharlau Chemicals (Barcelona, Spain) and used as received by the manufacturer.

The electrospinning process was used in the fabrication of pristine PMMA/PEO and dithioester-functionalized fibers of the type PMMA/PEO/DTE, as described in the following. First, PMMA and PEO were dissolved in chloroform (10 mL) at two different concentrations, i.e., 3 and 4% w/v. Subsequently, the DTE was added to the PMMA/PEO solution at a dosage equivalent to 5 and 10 wt % concerning the total polymer mass to obtain DTE-functionalized fibers thereinafter indicated as β, containing 5% wt DTE, and γ, containing 10% wt DTE, respectively. The DTE-free (namely, α fibers) fibers were also fabricated for comparison purposes. The mixtures were left to stir for 48 h at room temperature to obtain highly homogeneous solutions, which were then loaded into a glass syringe (10 mL volume) to be electrospun.

The electrospinning equipment included a spinneret with a metallic needle, a controlled-flow, four-channel volumetric microdialysis pump (KD Scientific, model: 789252), a high-voltage power source (10−50 kV, ES50P-20W Gamma High Voltage Research), and a custom-designed, grounded target collector, inside an interlocked safety cabinet. All electrospinning experiments were performed at 22 °C and 10−30% humidity, following specific electrospinning conditions (applied voltage: 10 kV, needle-to-collector distance: 30 cm, needle diameter: 18 G, and flow rate: 4.5 mL/h) that were found to be the optimum ones for these systems through a series of preliminary experiments. Depending on the polymer solution concentration, either "beads-on-string" (3 w/v%) or "beads-free" (4 w/v%) fiber morphologies were obtained, abbreviated in the following as α*, β*, and γ* and α, β, and γ, respectively.

2.2. EF Characterization. The morphological characterization of the DTE-free (α, α*) and the DTE-loaded (β, γ, β*, γ*) electrospun fibers before and after adsorption was carried out by scanning electron microscopy (SEM) using a Vega TS5136LS-Tescan. The samples were gold-sputtered (sputtering system K575X Turbo Sputter Coater, Emitech) before SEM inspection. Fiber average diameters were determined from the acquired SEM images using the software ImageJ.

Attenuated total reflectance spectroscopy (ATR) has been carried out using a Nicolet Instrument Nexus (Thermo Scientific, Waltham, MA, United States) for investigating the chemical stability of the produced EFs under acidic environments. For this purpose, the ATR spectra were recorded in the range of 4000−400 cm^{-1} for the as-prepared EFs and the corresponding materials after being immersed in acidic aqueous solutions (1 M HCl) at 25 and 50 °C.

Various material characterization methods were employed in this study to obtain information on the spent sorbents concerning their thermal stability, chemical composition, and morphology. More precisely, thermogravimetric analysis (TGA) was carried out to study the thermal stability of the material by using a Simultaneous Thermal Analyzer (STA) 6000 (PerkinElmer). During the test, the temperature was constantly increased with a specific heating rate. TGA was used to measure the variation in the mass of the exhausted sorbents over time and temperature. The temperature rose from 30 to 750 °C with a heating rate of 10 °C/min using an airflow rate of 40 mL/min.

Scanning electron microscopy (FEI INSPECT 12000x Electron Scanning Microscope) coupled with energy-dispersive X-ray spectroscopy (SEM-EDX) analysis was performed to observe the morphology of the fibers after the adsorption tests. Moreover, it was used to analyze the morphology of the ashes obtained after the TGA analyses and to qualitatively characterize their composition in terms of elemental constituents.

2.3. Adsorption Tests. The adsorption tests were designed to simulate acidic solutions derived from the hydrometallurgical treatment of palladium-loaded spent automotive catalysts carried out using hydrogen peroxide and hydrochloric acids, following a previously reported methodology.[42] The treatment of spent catalysts with such leaching solutions results in the complete consumption of hydrogen peroxides. The solutions are sometimes heated to favor the dissolution of the metal; however, the temperature is retained below certain levels to promote selective extraction of the desired metal ion (herein palladium). The spent solutions can be partially neutralized to favor the following refining step (e.g. adsorption) using sodium hydroxides. The residual solutions contain essentially chloride ions of the desired precious metal (herein palladium, with the dominant species being $PdCl_4^{-2}$), sodium chloride, and residual hydrochloric acid, usually above 0.01 M. The experiments were carried out in batch mode using PYREX-capped glass vials immersed in a water thermostatic bath to ensure constant temperature during the whole test duration. The test solutions were prepared by dissolving powdered palladium(II) nitrate dihydrate, $Pd(NO_3)_2{\cdot}2H_2O$ (MW 266.46 g/mol, 40 wt % of Pd(II), CAS number 32916-07-7, purchased from Sigma-Aldrich, Italy), in aqueous solutions containing hydrochloric acid and sodium chloride. The sample solutions were prepared using hydrochloric acid at different concentrations, obtained by dilution of hydrochloric acid (MW 36.46 g/mol, purity 37% w/w, CAS number 7647-01-0, purchased from Sigma-Aldrich, Italy) in deionized water. Sodium chloride, NaCl (MW: 58.44 g/mol, CAS number 7647-14-5, purchased by Honeywell, Germany), was also added to simulate the neutralization of the leaching solution and to test the effect of salinity on the adsorption process.

Equilibrium tests were performed for palladium in acidic conditions at three different HCl molarities equal to 1, 0.1, and 0.01 M. In particular, for each acid matrix, four different concentrations of Pd(II) from 10 to 80 mg/L were prepared (solution volume: 20 mL), in which the EF sorbents (m = 5 mg, beads-free or beads-on-string fibers) were immersed.

Adsorption tests in pure hydrochloric acid solutions have been carried out for both beads-free and beads-on-string morphologies at 20 and 50 °C. The effect of salinity has been investigated on beads-free fibers only, by adding NaCl to the acidic aqueous solutions. In particular, two sets of experiments were performed on α, β, and γ fibrous sorbents for a fixed Pd(II) concentration (60 mg/L) and fixed sorbent loading (m/V = 0.25 g/L) at 20 °C. In the first set, the HCl content was retained at 0.1 M and the total concentration of chloride ions was varied by adding NaCl up to 0.5M. The second set was carried out by keeping the total concentration of chloride ions at 0.5 M while varying the HCl and NaCl concentrations. A summary of the salinity effect tests is provided in Table 1.

Flame atomic absorption spectrophotometry (F-AAS) was used for the detection of palladium by operating at a wavelength of 340.5 nm and a gap amplitude of 1 mm (AAS, model SpectrAA 220, Varian Inc., Palo Alto, CA, United States). Calibration was carried out by

https://doi.org/10.1021/acsapm.4c00324
ACS Appl. Polym. Mater. 2024, 6, 9406−9419

Table 1. Salinity Effect Tests Performed at a Defined HCl Concentration while Varying [Cl^-] Ions by Adding NaCl and at a Retained [Cl^-] = 0.5 M while Varying HCl and NaCl Concentrations

Pd [mg/L]	HCl [M]	NaCl [M]	Cl^- [M]
60	0.1	0	0.1
60	0.1	0.05	0.15
60	0.1	0.1	0.2
60	0.1	0.25	0.35
60	0.1	0.35	0.45
60	0.1	0.4	0.5
60	0.1	0.5	0.6
60	0.2	0.3	0.5
60	0.3	0.2	0.5
60	0.4	0.1	0.5
60	0.5	0	0.5

preparing diluted samples starting from a standard palladium solution for atomic absorption spectroscopy (Sigma-Aldrich) having a calibrated concentration of 1000 ± 4 mg/L in 5% HCl. The solution pH of the test samples was measured using a pH meter, pH 50 V by XS instruments, or using standard acid−base titration methods, both at the beginning and the end of each test, after reaching equilibrium.

The uptake capacity of the sorbents in any matrix can be calculated from the mass balance according to eq 1:

$$q = (c_0 - c_{eq}) \cdot \frac{V}{m} \quad (1)$$

where q is the uptake capacity of the sorbent, [mg/g], c_0 is the initial palladium concentration, [mg/L], and c_{eq} is the palladium concentration after reaching equilibrium [mg/L].

3. RESULTS

3.1. EF Characterization. SEM images of selected samples of the as-prepared EFs are shown in Figure 1. As known from a previous study,[49] the polymer solution concentration is one of the most critical influencing parameters in electrospinning: by gradually increasing polymer solution concentration, the morphology of the produced materials changes gradually from collapsed particles and aggregates (electrospraying) to beads-on-string and finally to "beads-free" fibers.[50]

In our experiments, we noticed that 3% w/v polymer solutions gave rise to "beads-on-string" morphologies, whereas upon increasing the concentration to 4% w/v, homogeneous "beads-free" fibers with a regular morphology were obtained, in line with a recent publication of our group.[48] It is also clear that the "beads-on-string" morphology is characterized by much lower fiber diameters. More precisely, for the beads-free EFs, the average fiber diameters determined by using ImageJ were 4.390 ± 0.422 μm for α, 3.776 ± 0.272 μm for β, and 2.865 ± 0.307 μm for γ, whereas for the beads-on-strings EFs, average diameters of 0.528 ± 0.068 μm for α^*, 0.553 ± 0.130 μm for β^*, and 0.518 ± 0.117 μm for γ^* were recorded. SEM analysis also revealed that the diameter of the beads-free fibers decreased upon increasing the DTE content, while negligible

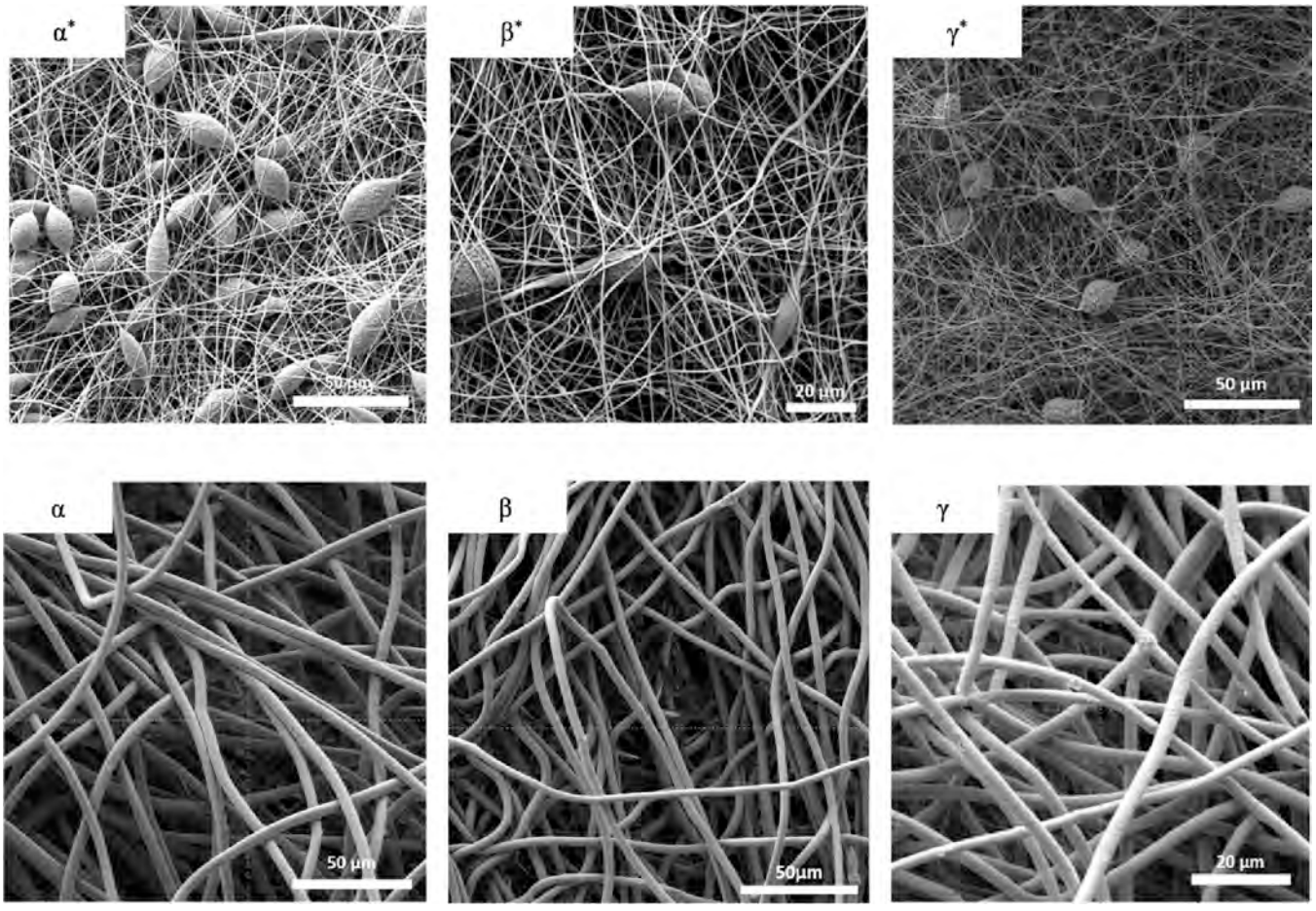

Figure 1. SEM images of the as-prepared electrospun fibrous adsorbents: α^*, β^*, and γ^* (beads-on-string) and α, β, and γ (beads-free).

https://doi.org/10.1021/acsapm.4c00324
ACS Appl. Polym. Mater. 2024, 6, 9406−9419

variations were observed in the case of the beads-on-string fibers.

To verify the chemical stability of the produced fibers upon immersion in acidic aqueous environments, the α-EFs ("beads-free", DTE-free) were analyzed by ATR before and after immersion in 1 M HCl at 25 and 50 °C for 48 h.

As seen in Figure 2, characteristic peaks corresponding to both polymers (PEO and PMMA) can be visualized. More precisely, the signals present between 3750 and 3000 cm^{-1} are attributed to the stretching vibrations of the −OH groups that are present in PEO, whereas the strong peak present at around 2884 cm^{-1} is associated with the −CH stretching modes. Moreover, the peaks present at around 1963 and 1342 cm^{-1} correspond to the −CH asymmetric bending and the $-CH_2$ wagging of PEO. Finally, the bands present at around 1100 cm^{-1} are attributed to the stretching vibrations of C−O−C, while the peaks at 960 and 840 cm^{-1} are associated with the $-CH_2-CH_2$ rocking and C−O−C vibration modes, respectively.[51,52] In the same spectrum, the broad signal present between 3100 and 2800 cm^{-1} corresponds to the stretching vibrations of the −CH bonds that are present in PMMA, while at 1724 cm^{-1}, the characteristic signal corresponding to the stretching mode of the C=O bonds of the ester groups can be seen. Additionally, the peak present at 1445 cm^{-1} can be assigned to the asymmetric stretching vibration of the $-CH_3$ group that is present in PMMA, while the stretching and bending of the C−O−C bonds are correlated to the peaks present at 1265 and 1145 cm^{-1}, respectively.[53,54] After the immersion of the EF in 1 M HCl at 25 and 50 °C, the characteristic signals corresponding to PEO (e.g., shown at ∼2884, 1963, 1100, and 1342 cm^{-1}) are diminished, suggesting its partial dissolution in the acidic solutions. In contrast, the characteristic signals of PMMA are retained after acid treatment at both temperatures, demonstrating the robustness and chemical stability of this polymer under test conditions.

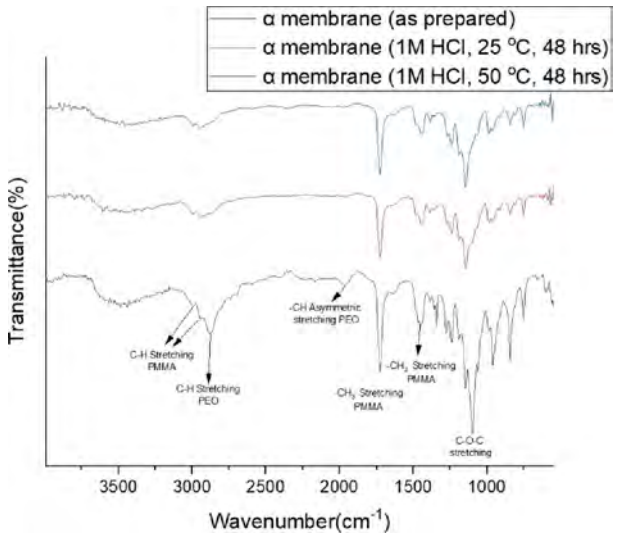

Figure 2. ATR spectra of the as-prepared α fibers (black line) and after immersion in 1 M HCl solution for 48 h at 25 °C (red line) and 50 °C (blue line).

In addition, the pH_{PZC} of each fibrous sorbent type was measured by immersing the EFs in deionized water (pH ≈ 5.4) and measuring the solution pH. The α membrane reached a value of pH_{PZC} = 8.5, the β membrane a value of pH_{PZC} = 6.15, while for the γ membrane, a pH_{PZC} = 5 was recorded. This demonstrates that the dithioester functional groups influence the solution pH. However, in the model solutions tested herein, any pH variations were recorded after adsorption.

EF TGA and SEM-EDX analysis were performed on the best-behaved γ fibers at [HCl] = 0.1 M and T = 20 °C. These tests are also useful to study a possible thermal recovery of Pd(II) from spent EFs, which is preferred here to chemical regeneration. The TGA curve of the γ fibrous membrane that adsorbed 80 mg/L palladium in 0.1 M HCl solution, for an adsorption time of 48 h, is shown in Figure 3a.

The main weight loss (90%) of the sample occurs in the range 200−350 °C, and the sample shows a total weight loss of 94% at the final temperature of 750 °C. The SEM-EDX analysis of the residual material, i.e., the ashes collected after the thermal treatment, is shown in Figure 3b, which indicates that metallic palladium is by far the dominant component of the ashes. The presence of silicon and oxygen also detected in the EDX is probably derived from the glass vials. This result suggests that thermal treatment of moderate severity (up to 400 °C) can be a useful strategy for the recovery of this precious metal from the adsorbent.

The TGA curve for the γ sample (100 mg/L), 0.1 M HCl, and 1 M NaCl solution (Figure 4a) shows a similar thermal

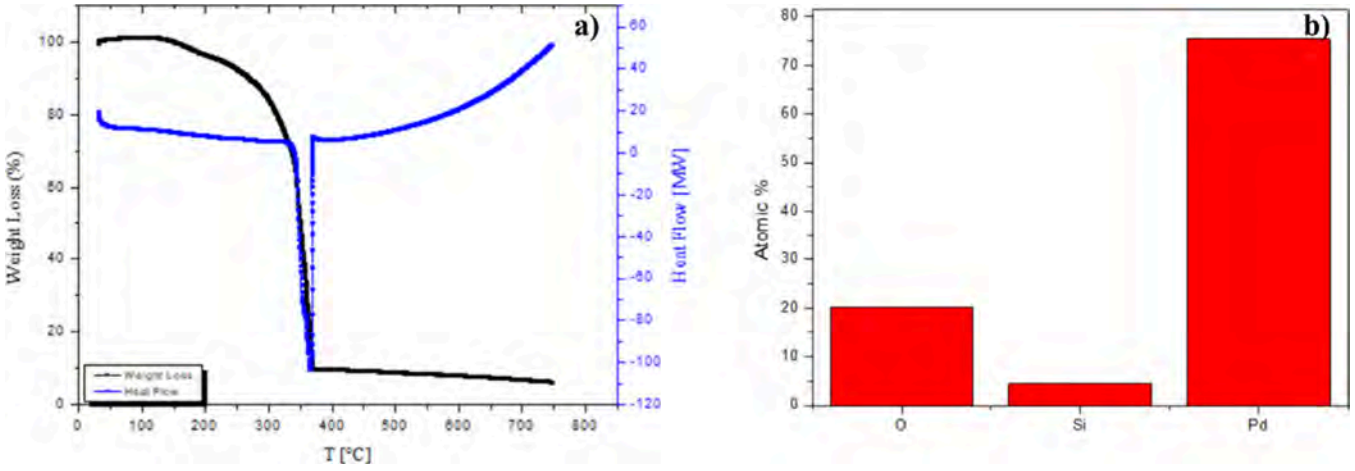

Figure 3. (a) TGA curve of γ that adsorbed 80 mg/L palladium in 0.1 M HCl. (b) EDX results of γ in 0.1 M HCl.

https://doi.org/10.1021/acsapm.4c00324
ACS Appl. Polym. Mater. 2024, 6, 9406−9419

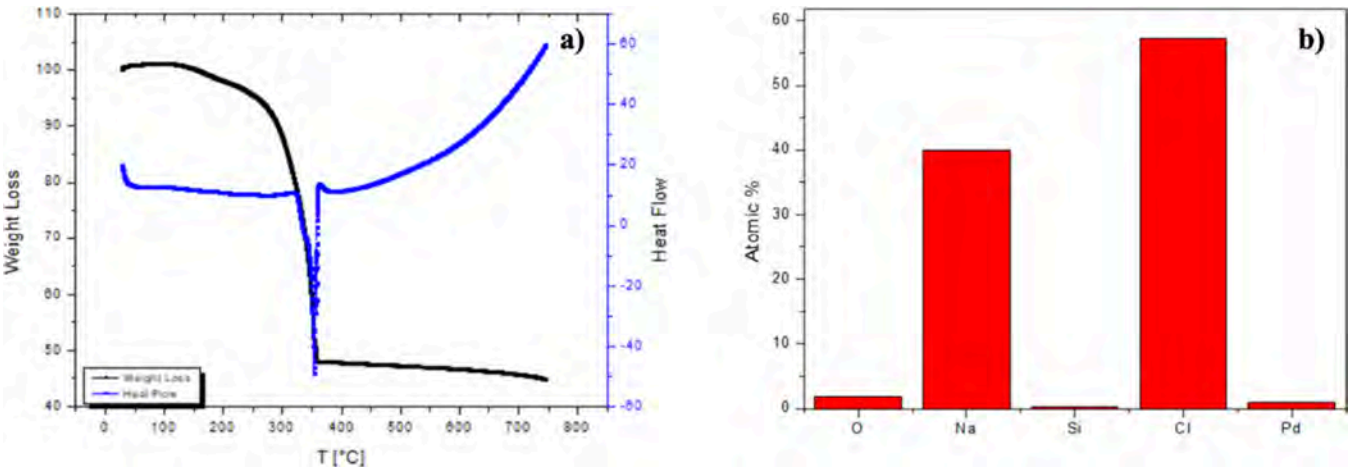

Figure 4. (a) TGA curve of γ in 0.1 M HCl−NaCl. (b) EDX results of γ in 0.1 M HCl−NaCl.

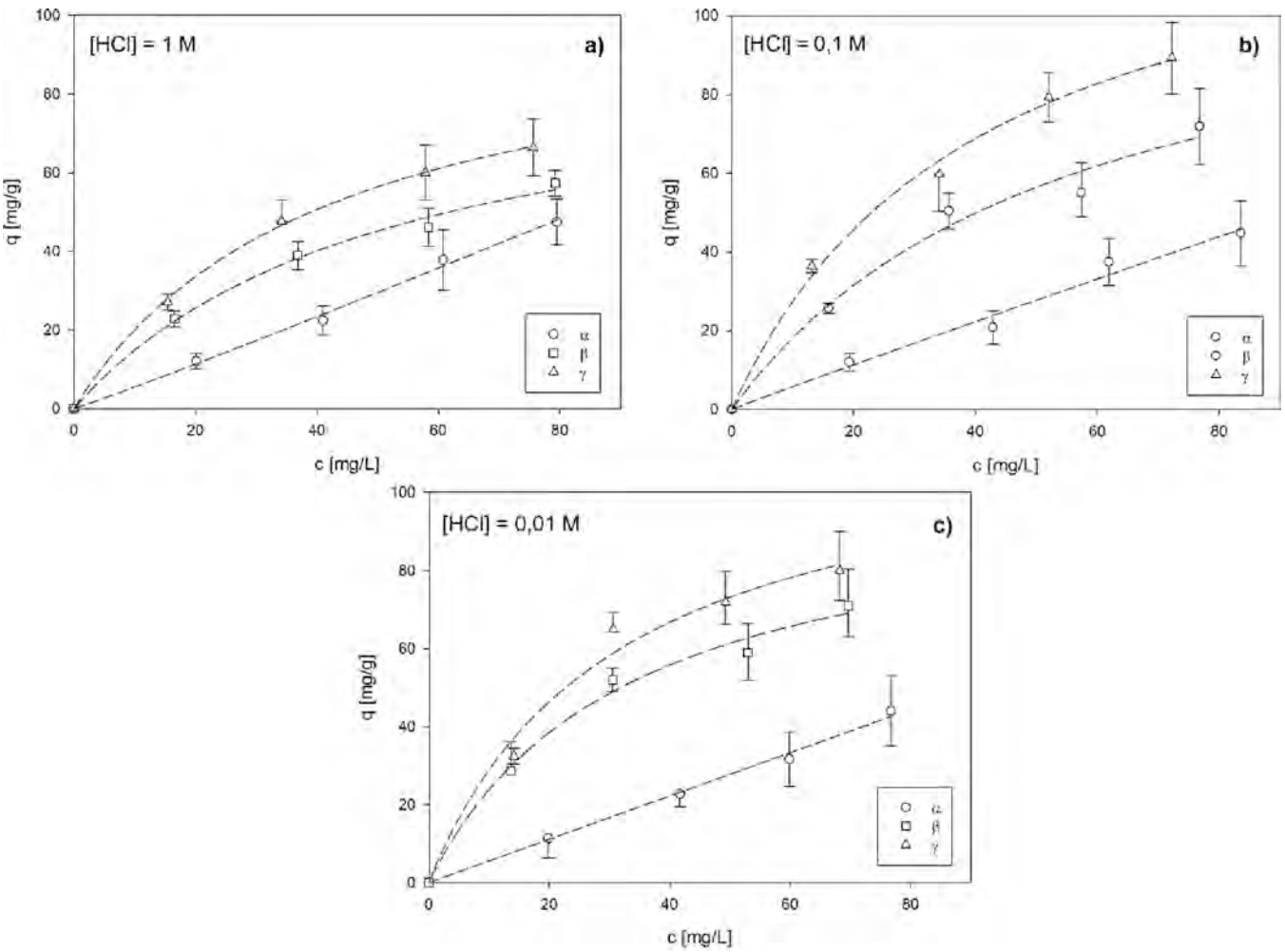

Figure 5. Adsorption isotherms for "beads-free" fibers at temperature = 20 °C for different concentrations of [HCl]: (a) 1 M, (b) 0.1 M, and (c) 0.01 M. The lines are only included for visualization purposes.

behavior, with a prevalent weight loss (57%) within 200−350 °C. Nevertheless, the total weight loss was only 55% at 750 °C.

The lower weight loss is attributed to the presence of NaCl. Water residues containing a large amount of NaCl remain over the spent EF, and upon heating, NaCl precipitates over the fibers. This is confirmed by EDX analysis of the ashes (Figure 4b). This problem could be overcome by repeated fiber rinsing to remove residual NaCl before the thermal recovery of Pd.

3.2. Adsorption Tests. Figures 5 and 6 depict the adsorption isotherms for the beads-free fibers (α, β, and γ) recorded at 20 and 50 °C for different HCl concentrations. It is noteworthy to mention that the solution pH is dominated by the high concentration of hydrochloric acid, so no alteration of

https://doi.org/10.1021/acsapm.4c00324
ACS Appl. Polym. Mater. 2024, 6, 9406−9419

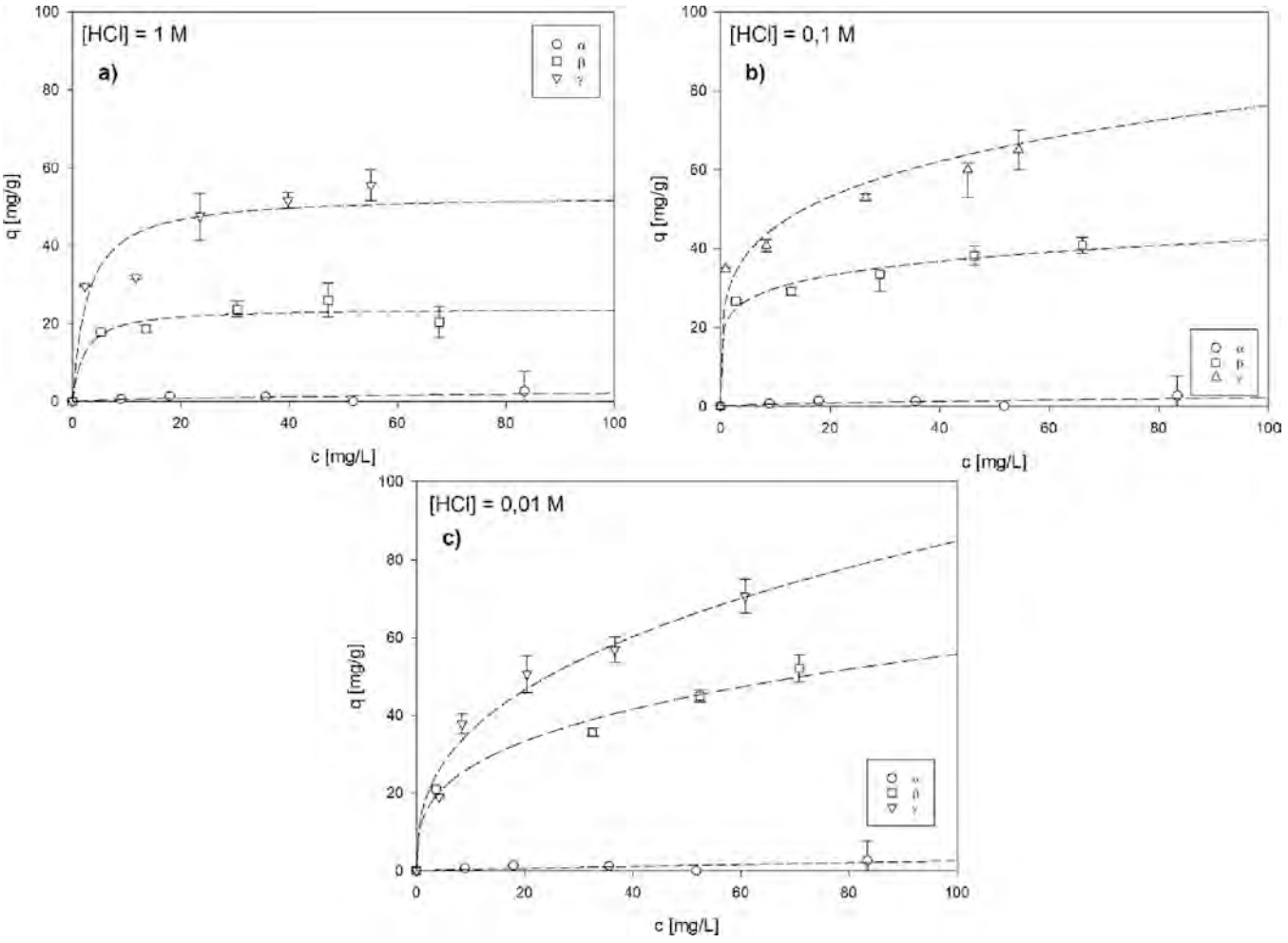

Figure 6. Adsorption isotherms for "beads-free" fibers at temperature = 50 °C for different concentrations of [HCl]: (a) 1 M, (b) 0.1 M, and (c) 0.01 M. The lines are guides for the eye.

the pH is observed before and after the tests due to palladium adsorption and EF hydrolysis.

As seen in Figure 5, for all HCl concentrations, the α fibers appear to have the lowest adsorption capacity, with the γ fibers being the most effective. Furthermore, at T = 20 °C, the isotherm for the α fibers showed a linear trend, while the others show a tendency toward saturation, which is however not achieved within the investigated concentration range.

The experiments also revealed that while in the case of the β and γ fibers, a pronounced effect of the HCl concentration on the adsorption efficiency was observed, this did not apply to the case of the α fibers, which showed an almost constant adsorption capability throughout the three different HCl concentrations.

Figure 6 shows that the adsorption capacity for the α fibers at 50 °C was negligible, while for the β and γ fibers, it was lower than that recorded at 20 °C for a high palladium concentration but higher for a palladium concentration below ~10 mg/L. Furthermore, the tendency to attain a saturation of adsorption capacity was more pronounced, especially as the HCl concentration increased.

Figures 7−9 compare the adsorption isotherms for the "beads-free" fibers (α, β, and γ) and the "beads-on-string" fibers (α*, β*, and γ*) for the HCl concentration levels at 20 °C. The experiments indicated that the adsorption capacity of the beads-free and the beads-on-string fibers do not differ significantly. At 0.1 M HCl, there is only a minor increase in the uptake capacity of the α* fibers compared to the α fibers and at 1 M HCl for the β*and γ* compared to the β and γ fibers. Furthermore, for the beads-on-string fibers, the adsorption capacity rises from α to γ, while asymptotic adsorption capacity is not reached for any of the three systems.

The effect of NaCl content on the adsorption performance of beads-free EFs can be seen in Figure 10. At a constant HCl content, the NaCl content has the sole effect of slightly reducing the adsorption capacity, with a more pronounced effect appearing from 0.2 to 0.35 M total chlorides (Figure 10a). At constant total chloride conditions (Figure 10b), a slight increase in adsorption capacity can be observed at an increased HCl concentration.

Table 2 summarizes the adsorption capacities of the EFs prepared in this study (recorded at T = 20 °C) and of other conventional sorbents at a reference Pd(II) concentration equal to 10 mg/L. As seen, for the majority of the sorbents listed in the literature, adsorption capacities less than 6 mg/g at c_0 = 10 mg/L have been reported, while only a handful of them reach 15 mg/g. Instead, the EFs developed in the present study show far better adsorption performances (especially the dithioester-functionalized β and γ fibers), reaching adsorption uptake values that are two or three times higher, comparable to that exhibited by the nanostructured magnetic composite Fe_3O_4@SiO_2−NH_2 proposed by Geng et al.[55] These findings

https://doi.org/10.1021/acsapm.4c00324
ACS Appl. Polym. Mater. 2024, 6, 9406−9419

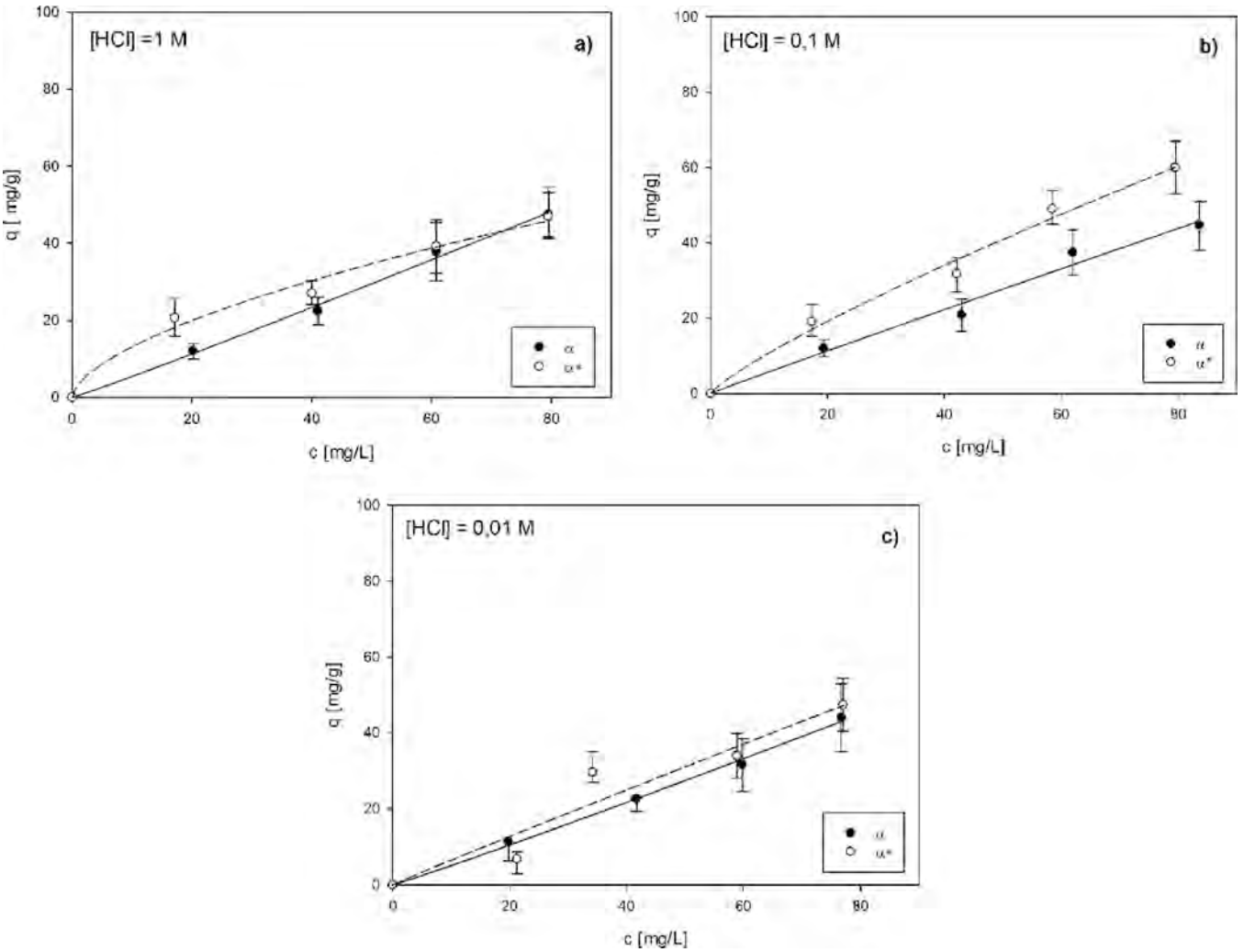

Figure 7. Comparison between "beads-free" α and "beads-on-string" α* fiber adsorption isotherms at temperature = 20 °C for different concentrations of [HCl]: (a) 1 M, (b) 0.1 M, and (c) 0.01 M. The lines are only included for visualization purposes.

demonstrate that the proposed EFs can be a suitable option for palladium recovery in hydrometallurgical refining processes.

3.3. Adsorption Process Modeling. Several classical models (e.g., Henry, Freundlich, Temkin and Langmuir) can be used for the interpretation of the adsorption isotherms provided in Figures 3−7. Considering the chemical characteristics of the α sorbent and the shape of the corresponding adsorption isotherms, it is expected that Pd(II) adsorption takes place on a dominant kind of active site for the α fibers. This can be recognized in the esther group of PMMA, which can interact directly with Pd(II) ions or through geminal diols forming by its hydrolysis in acidic solutions.

In the DTE-loaded fibers, DTE functional groups further contribute to the adsorption process, and consequently, multiple adsorption sites are required to describe the adsorption isotherms. Besides, it is also worth remembering that palladium speciation in the conditions investigated herein indicates the predominance of $PdCl_4^{-2}$ anion: the concentration of this ion reflects the total concentration of palladium in solution. Among the classical adsorption models, Langmuir's model is the one that assures more flexibility in describing this kind of situation.

The adsorption of a single ion on a sorbent characterized by a single active site as described by Langmuir's model is given by eq 2:

$$q_{eq} = q_{MAX}\frac{K\cdot c_{eq}}{1 + K\cdot c_{eq}} \quad (2)$$

where q_{MAX} is the maximum uptake capacity of the sorbent, [mg/g], proportional to the concentration of the active sites; K is the thermodynamic equilibrium constant for the ion-active site interaction, a known function of the standard Gibbs free energy ΔG^0, universal gas constant R, and temperature, T [K], as shown in eq 3[63,64]

$$K = \exp\left(-\frac{\Delta G^0}{RT}\right) \quad (3)$$

While the existence of a single active site is not always common, the existence of a "dominant" class of active sites over the many available on the sorbent surface is more frequent. In this case, Langmuir's model provides information on the overall concentration of the dominant active sites and their average standard Gibbs free energy of interaction with the ion. When multiple distinct classes of active sites are relevant, the adsorption isotherm can be well described under the

https://doi.org/10.1021/acsapm.4c00324
ACS Appl. Polym. Mater. 2024, 6, 9406−9419

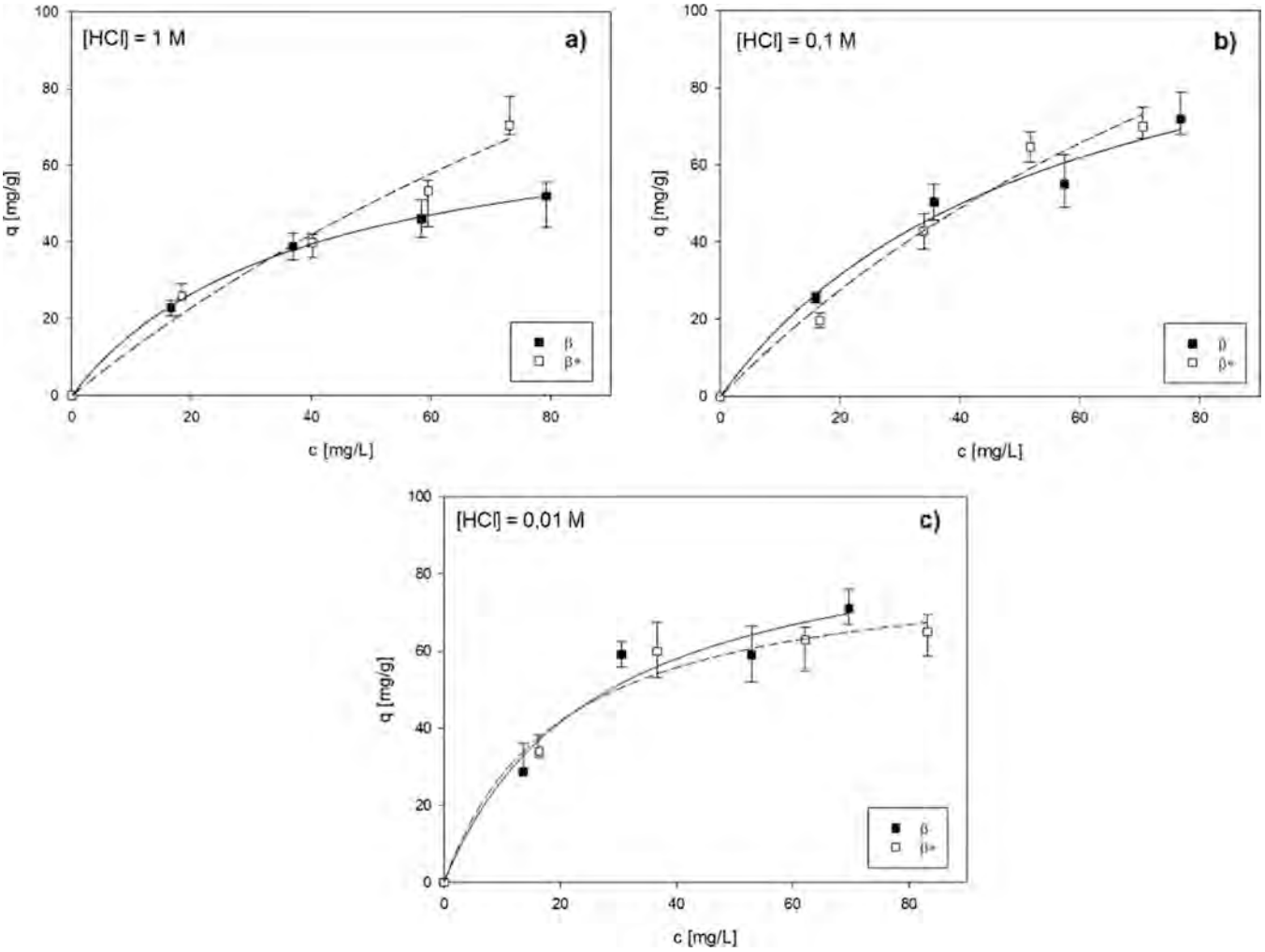

Figure 8. Comparison between "beads-free" β and "beads-on-string" β* fiber adsorption isotherms at temperature = 20 °C for different concentrations of [HCl]: (a) 1 M, (b) 0.1 M, and (c) 0.01 M. The lines are only included for visualization purposes.

Langmuir model as the summation of the adsorption isotherms of each single class of active sites.

An almost linear trend of the adsorption isotherms, as that observed for the α fibers, can be seen as the first part of the Langmuir isotherm, at low ion concentrations, i.e.,

$$q_{eq} = H \cdot c_{eq} \cong q_{MAX,\alpha} K \cdot c_{eq} \quad (4)$$

Before testing Langmuir's model, it is also worth observing that the α and α* fibers have the same chemical composition but different morphology. The different surface areas of the α and α* fibers are responsible for the different tendencies of these two sorbents to approach different saturation conditions ($q = q_{MAX}$).

Since the chemistry of α and α* fibers is the same, the equilibrium constants for the two fibers, K, and the corresponding value of the Gibbs free energy, ΔG^0, are thought to be the same, while different values of q_{MAX} ($q_{MAX,\alpha}$ and q_{MAX,α^*}) are expected. Global fitting of the experimental data has been carried out (using SigmaPlot 14.0 software), assuming that the value of the parameter ΔG^0 is the same for both α and α*. The best fitting is obtained with $\Delta G^0 = -13850 \pm 73.77$ J/mol, $q_{MAX,\alpha} = 234.02 \pm 9.24$ mg/g, and $q_{MAX,\alpha^*} = 299.28 \pm 10.39$ mg/g. The determination factor R^2 of the overall fitting is 92.25%.

The model analysis revealed that the α* fibers can potentially lead to a higher maximum adsorption capacity, q_{MAX}, compared to the α fibers. This result can be explained by considering the morphology of the fibers, as shown in Figure 1. While, on the one hand, the beads-on-string configuration is characterized by the presence of spherules within the fibrous mat that accumulate a large mass of polymer in a limited surface area, on the other hand, the fibers' diameters are much smaller than those achieved with the beads-free configuration. Overall, the surface area of the beads-free α fibers can be estimated as around 0.79 ± 0.08 m^2/g, considering the average fiber diameter derived from image analysis (4.39 ± 0.42 μm) and the polymer density (nearly 1034 kg/m^3). In the case of the α* mat, a surface area of around 7.34 ± 0.8 m^2/g was calculated for the single fibers, while that of the α* beads was found to be nearly 0.30 ± 0.08 m^2/g. Assuming that the total surface area of the fibers is proportional to the value of q_{MAX}, the surface area of α* can be determined by multiplying $q_{MAX,\alpha^*}/q_{MAX,\alpha}$ with the value of the surface area of the α fibers.

This corresponds to nearly 88% of the α* fiber mass accumulated in the beads or, equivalently, nearly 74% of the surface area concentrated in the fibers. This is consistent with the image analysis of the α* fibers, from which it appears that the beads represent 15−35% of the observed area of the fibrous mat, as shown in Figure 1.

https://doi.org/10.1021/acsapm.4c00324
ACS Appl. Polym. Mater. 2024, 6, 9406−9419

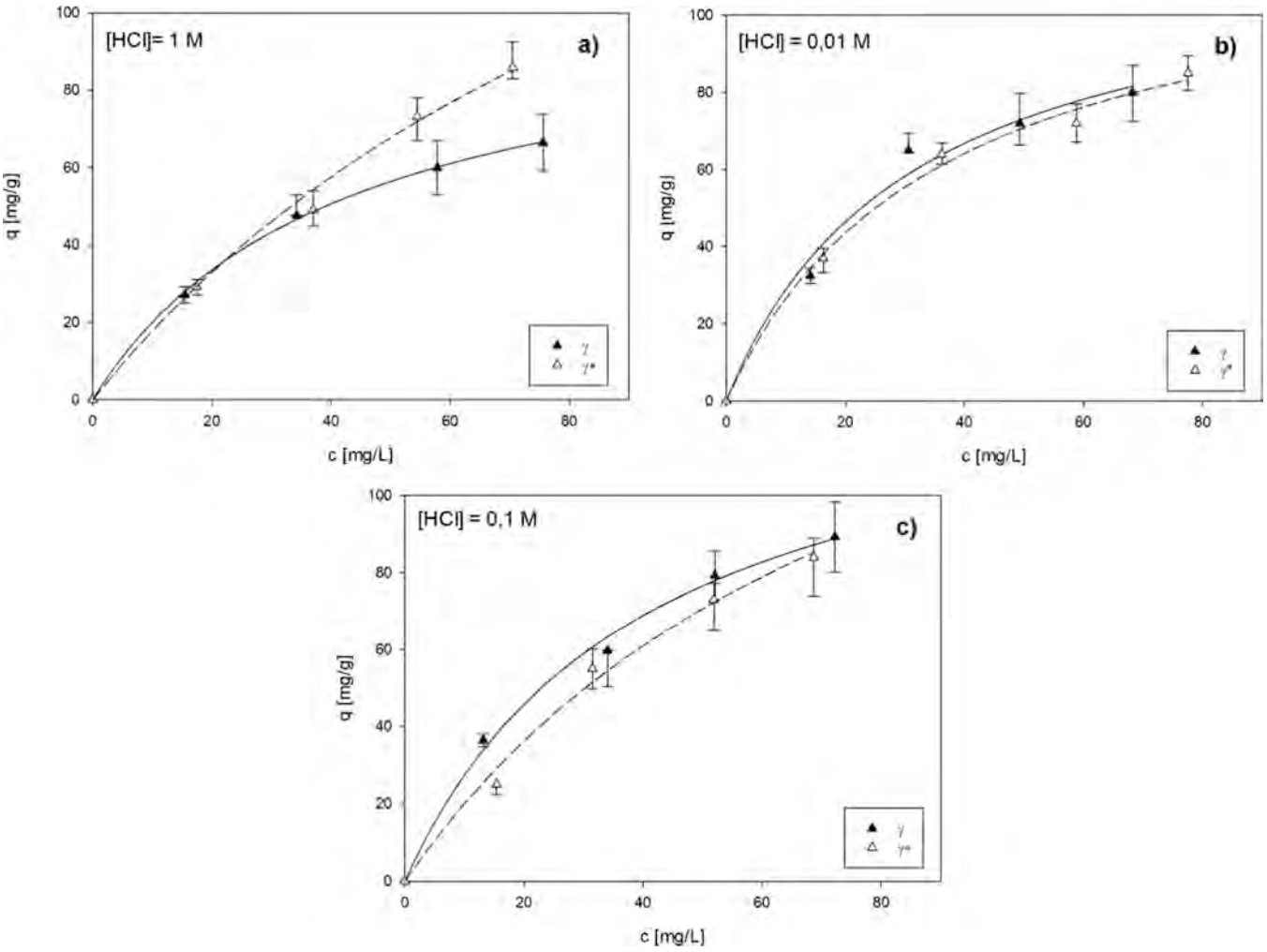

Figure 9. Comparison between "beads-free" γ and "beads-on-string" γ* fiber adsorption isotherms at temperature = 20 °C for different concentrations of [HCl]: (a) 1 M, (b) 0.1 M, and (c) 0.01 M. The lines are only included for visualization purposes.

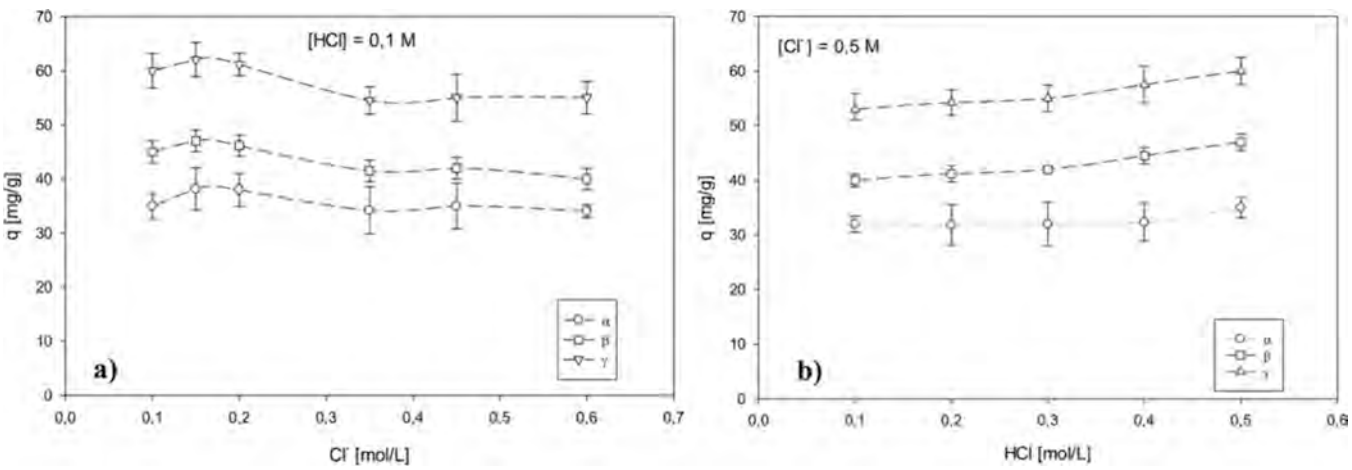

Figure 10. (a) Effect of [Cl^-] on the adsorption capacity of "beads-free" fibers at [HCl] = 0.1 M. (b) Effect of [HCl] on the adsorption capacity of "beads-free" fibers by retaining the chloride ion concentration at 0.5 M.

In contrast, Langmuir's adsorption model cannot be used to describe β (β*) and γ (γ*) fibers. Indeed, the experiments indicate that the presence of DTE increases the adsorption capacity in proportion to the amount of DTE added to the fibers. However, the increase in adsorption capacities is not linear: doubling the quantity of DTE does not result in doubled adsorption capacities. Figures 3 and 4 demonstrate that the difference in β (β*) and γ (γ*) uptake capacities lowers at concentration levels of 10−20 mg/L while reaching an almost constant value for higher concentrations. This suggests that the active sites of β and γ attain saturation adsorption capacity at palladium concentrations below 20 mg/

https://doi.org/10.1021/acsapm.4c00324
ACS Appl. Polym. Mater. 2024, 6, 9406−9419

Table 2. Adsorption Capacities of Different Sorbent Pd(II) Concentrations of 10 mg/L

sorbent	solvent	T [°C]	q [mg/g] at 10 mg/L	ref
Fe_3O_4@SiO_2-NH_2	[HCl]: 0.25 M	25	50	55
γ	[HCl]: 0.01 M	20	37	this work
β	[HCl]: 0.01 M	20	30	this work
MOF-802	[HCl]: 0.1 M	25	17.3	56
beads (sericin, alginate, and PEGDE)	[HNO_3], [NaOH]: pH = 2.5	55	16	57
α	[HCl]: 1, 0.1, 0.01 M	20	8	this work
MOF-808	[HCl]: 0.1 M	25	2.61	56
CA (Norit GF 40)	[HCl]: 0.1 M	21	5	58
silk fibroin fiber	water: pH ≈ 7	25	3	59
UiO-66	[HCl]: 0.1 M	25	5.63	56
Aspergillus sp.	[HNO_3], [NaOH]: pH = 3.5	25	1.7	60
Ch-DB18C6	[HCl]: 0.1 M	25	1	61
Lewatit TP-214 resin	[HCl]: 0.0032 M	25	0.5	62

L. At 50 °C, the β and γ behavior depends more on pH, and while a saturation can be given at 0.1 and 1 M HCl, an increase in the adsorption capacity can be seen at 0.01 M. The average value of this DTE saturation adsorption capacity (q_{MAX}^{DTE}) can be estimated as the average increase in the capture capacities of β and γ fibers over α fibers at a concentration above 20 mg/L, as shown in Table 3, which also reports a comparison of the ratio between $q_{MAX}^{DTE}(\gamma)$ and $q_{MAX}^{DTE}(\beta)$ at 20 and 50 °C.

Table 3. Average Increase in Capture Capacity for β and γ Fibers

EF	T [°C]	q_{MAX}^{DTE}	[HCl] = 1 M	[HCl] = 0.1 M	[HCl] = 0.01 M
β	20	mean	13.08	26.54	34.40
		std error	1.451	2.082	4.099
	50	mean	13.00	22.44	30.99
		std error	0.784	0.619	3.030
γ	20	mean	21.65	43.65	44.14
		std error	2.965	4.990	2.914
	50	mean	34.89	43.02	46.90
		std error	3.149	2.952	4.570
$q_{MAX}^{DTE}(\gamma)/q_{MAX}^{DTE}(\beta)$ at 20 °C			1.656	1.645	1.283
$q_{MAX}^{DTE}(\gamma)/q_{MAX}^{DTE}(\beta)$ at 50 °C			2.684	1.917	1.514

At T = 20 °C, the average increase in the adsorption capacity for γ is almost 50% greater than that of β, while at T = 50 °C, it increases with the HCl content from 50 to 150%. Moreover, it can be noticed that in most of the operating conditions, the average increase in the capture capacity passing from α to β and γ fibers is scarcely affected by the temperature, while for γ fibers at [HCl] = 1 M, it highly increased passing from 20 to 50 °C.

Finally, Table 4 shows the ratio between the maximum amount of adsorbed Pd(II) ions (mol_{Pd}) and the moles of DTE present on the fiber (mol_{DTE}). The experimental results indicate that not all of the DTE functional groups are accessible to Pd(II). Given the DTE saturation effect observed from the adsorption isotherm, this result can be considered as a clear indication of the fraction of DTE, which effectively resides over the surfaces of the fibers. For β fibers, this fraction is around 40−60% on average, while for γ, this is below 35%. Higher HCl concentrations correspond to lower DTE saturation (see Table 4) and a lower fraction of used DTE. The overall exothermic nature of adsorption processes can explain why these values slightly reduce with the temperature.

Table 4. Ratio between the Moles of Pd(II) Adsorbed on the Fibers and the Moles of the DTE Functional Groups Present on the Fibers

		% DTE saturation (mol_{Pd}/mol_{DTE})		
EF	T [°C]	[HCl] = 1 M	[HCl] = 0.1 M	[HCl] = 0.01 M
β	20	46.6%	59.2%	65.1%
	50	31.1%	41.5%	48.2%
γ	20	28.6%	38.5%	34.8%
	50	30.4%	34.6%	32.6%

4. CONCLUSIONS

In this work, the recovery of palladium from hydrochloric acid model solutions was meticulously pursued, employing adsorption, utilizing electrospun fibers (EFs) comprised of PMMA and PEO with two different morphologies: "beads-free" (α, β, and γ) and "beads-on-string" (α*, β*, and γ*). The β and the β* fibers were produced by doping 5% wt DTE in the PMMA−PEO matrix, while the γ and γ* fibers were produced with 10% wt DTE. Based on the HSAB principle, where soft acids rich in S or N donor atoms exhibit strong affinity with Pd (II) ions, the incorporation of dithioester functionalities facilitates complexation with soft species such as the $PdCl_4^{2-}$ dissolved in solution.

A meticulous construction of adsorption isotherms ensued for each thermodynamic trial run on palladium solutions, unraveling several noteworthy revelations.

A nearly 25% difference in the adsorption capacity of "beads-on-string" and "beads-free" α fibers was observed, with the performances of the α* being slightly higher due to the higher surface area of these fibers. Both the α and the α* fibers are scarcely affected by the HCl content, whereas β and γ fibers exhibited enhanced adsorption capacities at HCl concentrations of 0.1 and 0.01 M, compared to 1 M HCl. Notably, at 20 °C and 0.1 M HCl, γ demonstrated a maximum adsorption capacity (q = 100 mg/g at 80 mg/L), surpassing β (q = 70 mg/g) and α (q = 50 mg/g). None of the fibers achieved an asymptotic adsorption capacity within the investigated concentration range (10−80 mg/L).

At 50 °C, β and γ have superior performance compared to α, exhibiting a propensity to attain a q_{MAX} asymptotic value at low concentration levels (10 mg/L). This maximum adsorption capacity at 50 °C is almost 20−30 mg/g lower than the corresponding adsorption capacities shown at 20 °C, confirming the exothermic nature of adsorption processes.

The introduction of chloride ions upon NaCl addition either at constant acidity or constant total chloride concentration marginally affects the performance of all three fibers. The comparison with other conventional sorbents available in the pertinent literature for palladium recovery indicated that γ emerged as the preeminent fibrous adsorbent, particularly in 0.1 M HCl solution, thereby corroborating the substantial enhancements conferred by DTE functionalization.

https://doi.org/10.1021/acsapm.4c00324
ACS Appl. Polym. Mater. 2024, 6, 9406−9419

Experiments of the thermal treatment of the Pd-loaded fibers also revealed the absence of chlorides associated with the adsorbed palladium ions, suggesting that the overall process involves chemical reactions either consisting in the reduction of Pd(II) to Pd(0) or the transformation of $PdCl_4^{-2}$ ions into new Pd(II) complexes with the surface functional groups. The low temperatures required for the thermal recovery is another noticeable advantage of the fibers since this provides a valuable route to recover solid palladium from a hydrometallurgic process.

Finally, the β and γ fibers show adsorption capacities that mirror the presence of two distinct contributions: the intrinsic adsorption capacity of the polymeric PEO−PMMA matrix (as for the α fibers) and the complexation with the DTE present on the fibers, which is completed already at concentrations close to 10−20 mg/L. The appreciable performances of the proposed materials and the possibilities offered by electrospinning in producing fibers with tailored chemical structures and morphology and an easy thermal recovery of the metal indicate that this new method to produce sorbents is worth further research efforts.

AUTHOR INFORMATION

Corresponding Author

Luigi Piero Di Bonito − *Dipartimento di Matematica e Fisica, Università degli Studi della Campania "Luigi Vanvitelli", 81100 Caserta, Italy; Dipartimento di Ingegneria Chimica, dei Materiali e della Produzione Industriale Intensification of Separation Processes for the Environment and the Circular Economy Laboratory (STEEL), Università degli Studi di Napoli "Federico II", 80125 Napoli, Italy;* orcid.org/0000-0001-5002-4789; Email: luigipiero.dibonito@unicampania.it

Authors

Paraskevas Kyriacou − *Department of Mechanical and Manufacturing Engineering, University of Cyprus, 2103 Nicosia, Cyprus*

Antonio Di Colandrea − *Dipartimento di Ingegneria Chimica, dei Materiali e della Produzione Industriale Intensification of Separation Processes for the Environment and the Circular Economy Laboratory (STEEL), Università degli Studi di Napoli "Federico II", 80125 Napoli, Italy*

Francesco Di Natale − *Dipartimento di Ingegneria Chimica, dei Materiali e della Produzione Industriale Intensification of Separation Processes for the Environment and the Circular Economy Laboratory (STEEL), Università degli Studi di Napoli "Federico II", 80125 Napoli, Italy*

Giovanna Ruoppolo − *National Research Council, Institute of Sciences and Technologies for Sustainable Energy and Mobility, CNR-STEMS, 80125 Napoli, Italy*

Theodora Krasia-Christoforou − *Department of Mechanical and Manufacturing Engineering, University of Cyprus, 2103 Nicosia, Cyprus*

Complete contact information is available at: https://pubs.acs.org/10.1021/acsapm.4c00324

Notes

The authors declare no competing financial interest.

ACKNOWLEDGMENTS

The authors sincerely thank Eng. Colomba Sorrentino and Eng. Silvia Vasaturo for their support in the research activities and Dr. Luciano Cortese (National Research Council, Institute of Sciences and Technologies for Sustainable Energy and Mobility, CNR-STEMS, Piazzale Tecchio, 80, 80125 Napoli, Italia) for his support in SEM-EDX analysis. This work was financed by European Community-NEXT Generation EU through the Ministero dell'Università e della Ricerca (MUR), Fondo per il Programma Nazionale di Ricerca e Progetti di Rilevante Interesse Nazionale (PRIN), Green and Sustainable Urban Mining of Noble Metals (DURABLE Project) [grant nos. P2022RF4Z7; CUP E53D2301743 0001].

REFERENCES

(1) Savva, I.; Krasia-Christoforou, T.; Kny, E.; Ghosal, K.; Thomas, S.; Savva, I. S.; Krasia-Christoforou, T.; Thomas, S.; Ghosal, K.; Kny, E.; "Encroachment of Traditional Electrospinning." in *Electrospinning − Basic Research to Commercialization* (Eds.;), ISBN: 978−1-78801−100−6, Royal Society of Chemistry, 2018 Chapter 2, 24−54.

(2) Venezia, V.; Prieto, C.; Evtoski, Z.; Marcoaldi, C.; Silvestri, B.; Vitiello, G.; Luciani, G.; Lagaron, J. M. Electrospun Hybrid TiO2/Humic Substance PHBV Films for Active Food Packaging Applications. *J. Ind. Eng. Chem.* **2023**, *124*, 510.

(3) Campardelli, R.; Pettinato, M.; Drago, E.; Perego, P. Production of Vanillin-Loaded Zein Sub-Micron Electrospun Fibers for Food Packaging Applications. *Chem. Eng. Technol.* **2021**, *44* (8), 1390−1396.

(4) Szewczyk, P. K.; Kopacz, M.; Krysiak, Z. J.; Stachewicz, U. Oil-Infused Polymer Fiber Membranes as Porous Patches for Long-Term Skin Hydration and Moisturization. *Macromol. Mater. Eng.* **2024**, *309* (2), 2300291 DOI: 10.1002/mame.202300291.

(5) Karbowniczek, J. E.; Berniak, K.; Knapczyk-Korczak, J.; Williams, G.; Bryant, J. A.; Nikoi, N. D.; Banzhaf, M.; de Cogan, F.; Stachewicz, U. Strategies of Nanoparticles Integration in Polymer Fibers to Achieve Antibacterial Effect and Enhance Cell Proliferation with Collagen Production in Tissue Engineering Scaffolds. *J. Colloid Interface Sci.* **2023**, *650*, 1371−1381.

(6) Knapczyk-Korczak, J.; Ura, D. P.; Gajek, M.; Marzec, M. M.; Berent, K.; Bernasik, A.; Chiverton, J. P.; Stachewicz, U. Fiber-Based Composite Meshes with Controlled Mechanical and Wetting Properties for Water Harvesting. *ACS Appl. Mater. Interfaces* **2020**, *12* (1), 1665−1676, DOI: 10.1021/acsami.9b19839.

(7) Knapczyk-Korczak, J.; Szewczyk, P. K.; Ura, D. P.; Bailey, R. J.; Bilotti, E.; Stachewicz, U. Improving Water Harvesting Efficiency of Fog Collectors with Electrospun Random and Aligned Polyvinylidene Fluoride (PVDF) Fibers. *Sustainable Mater. Technol.* **2020**, *25*, No. e00191, DOI: 10.1016/j.susmat.2020.e00191.

(8) Uddin, Z.; Ahmad, F.; Ullan, T.; Nawab, Y.; Ahmad, S.; Azam, F.; Rasheed, A.; Zafar, M. S. Recent Trends in Water Purification Using Electrospun Nanofibrous Membranes. *Int. J. Environ. Sci. Technol.* **2022**, 9149−9176, DOI: 10.1007/s13762-021-03603-9.

(9) Salehi, M.; Sharafoddinzadeh, D.; Mokhtari, F.; Esfandarani, M. S.; Karami, S. Electrospun Nanofibers for Efficient Adsorption of Heavy Metals from Water and Wastewater. *Clean Technologies and Recycling* **2021**, *1* (1), 1−33.

(10) Xu, X.; Lv, H.; Zhang, M.; Wang, M.; Zhou, Y.; Liu, Y.; Yu, D. G. Recent Progress in Electrospun Nanofibers and Their Applications in Heavy Metal Wastewater Treatment. *Front. Chem. Sci. Eng.* **2023**, 249 DOI: 10.1007/s11705-022-2245-0.

(11) Chen, H.; Huang, M.; Liu, Y.; Meng, L.; Ma, M. Functionalized Electrospun Nanofiber Membranes for Water Treatment: A Review. *Sci. Total Environ.* **2020**, No. 139944, DOI: 10.1016/j.scitotenv.2020.139944.

(12) Pereao, O.; Bode-Aluko, C.; Laatikainen, K.; Nechaev, A.; Petrik, L. Morphology, Modification and Characterisation of Electrospun Polymer Nanofiber Adsorbent Material Used in Metal Ion Removal. *J. Polym. Environ.* **2019**, 1843−1860, DOI: 10.1007/s10924-019-01497-w.

(13) Kumar Shetty, M.; Karthik, K. V.; Patil, J. H.; Murthy Shekhar, S.; Desai, S. M.; Hiremath, P. G.; Ravishankar, R. Sorption Studies of

Cr (VI) Ions from Synthetic Waste Water Using Chitosan Embedded in Calcium Alginate Beads. *Mater. Today Proc.* **2023**, *76*, 1.
(14) Mohammed, Y. A. Y. A.; Abdel-Mohsen, A. M.; Zhang, Q.-J.; Younas, M.; Zhong, L.-B.; Yang, J.-C. E.; Zheng, Y.-M. Facile Synthesis of ZIF-8 Incorporated Electrospun PAN/PEI Nanofibrous Composite Membrane for Efficient Cr(VI) Adsorption from Water. *Chem. Eng. J.* **2023**, *461*, No. 141972, DOI: 10.1016/j.cej.2023.141972.
(15) Pearson, R. G. Hard and Soft Acids and Bases. *J. Am. Chem. Soc.* **1963**, 3533 DOI: 10.1021/ja00905a001.
(16) Alfarra, A.; Frackowiak, E.; Béguin, F. The HSAB Concept as a Means to Interpret the Adsorption of Metal Ions onto Activated Carbons. *Appl. Surf. Sci.* **2004**, *228* (1−4), 84−92.
(17) Li, L.; Guo, W.; Zhang, S.; Guo, R.; Zhang, L. Electrospun Nanofiber Membrane: An Efficient and Environmentally Friendly Material for the Removal of Metals and Dyes. *Molecules* **2023**, 3288 DOI: 10.3390/molecules28083288.
(18) Song, K. S.; Coskun, A. Porous Organic Polymers for Selective Palladium Recovery and Heterogeneous Catalysis. *Chimia (Aarau)* **2023**, *77* (3), 122−126.
(19) Pandey, A.; Kalamdhad, A.; Chandra Sharma, Y. Recent Advances of Nanocellulose as Biobased Adsorbent for Heavy Metal Ions Removal: A Sustainable Approach Integrating with Waste Management. *Environ. Nanotechnol., Monit. Manage.* **2023**, No. 100791, DOI: 10.1016/j.enmm.2023.100791.
(20) Di Bonito, L. P.; Kyriacou, P.; Di Natale, F.; Krasia-Christoforou, T. Design and Production of Functionalized Electrospun Nanofibrous Membranes for Water Treatments. *Sci. Total Environ.* **2023**, No. 139944, DOI: 10.1016/j.scitotenv.2020.139944.
(21) Papaphilippou, P. C.; Karamanis, P.; Stavrinou, K.; Krasia-Christoforou, T. Functionalized Electrospun Fibrous Membranes as Effective Adsorbents for Benzoic Acid from Aqueous Media. *ChemistrySelect* **2020**, *5* (29), 9017−9021.
(22) Panteli, S.; Savva, I.; Efstathiou, M.; Vekas, L.; Marinica, O. M.; Krasia-Christoforou, T.; Pashalidis, I. *β*-Ketoester-Functionalized Magnetoactive Electrospun Polymer Fibers as Eu(III) Adsorbents. *SN Appl. Sci.* **2019**, *1* (1), 1 DOI: 10.1007/s42452-018-0034-7.
(23) Christou, C.; Philippou, K.; Krasia-Christoforou, T.; Pashalidis, I. Uranium Adsorption by Polyvinylpyrrolidone/Chitosan Blended Nanofibers. *Carbohydr. Polym.* **2019**, *219*, 298−305.
(24) Philippou, K.; Christou, C. N.; Socoliuc, V.; Vekas, L.; Tanasă, E.; Miclau, M.; Pashalidis, I.; Krasia-Christoforou, T. Superparamagnetic Polyvinylpyrrolidone/Chitosan/Fe3O4 Electrospun Nanofibers as Effective U(VI) Adsorbents. *J. Appl. Polym. Sci.* **2021**, *138* (15), 50212 DOI: 10.1002/app.50212.
(25) Liu, J.; Jin, C.; Wang, C. Hyperbranched Thiourea-Grafted Electrospun Polyacrylonitrile Fibers for Efficient and Selective Gold Recovery. *J. Colloid Interface Sci.* **2020**, *561*, 449−458.
(26) Iqbal, A.; Jan, M. R.; Shah, J.; Rashid, B. Recovery of Critical Metals from Leach Solution of Electronic Waste Using Magnetite Electrospun Carbon Nanofibres Composite. *Environmental Science and Pollution Research* **2022**, *29* (59), 88763−88778.
(27) Zeytuncu-Gökoğlu, B.; Şengür Taşdemir, R.; Tanç, B.; Aktaş, S.; Koyuncu, İ. Recycling of Precious Materials by Modified Electrospun Membranes. *Desalination Water Treat.* **2021**, *211*, 439−447.
(28) Wang, S. H.; Chang, F. C. Cu(II) and Au(III) Recovery with Electrospun Lignosulfonate CO2-Activated Carbon Fiber. *Int. J. Biol. Macromol.* **2022**, *203*, 505−514.
(29) Hao, J.; Wang, Y.; Wu, Y.; Guo, F. Metal Recovery from Waste Printed Circuit Boards: A Review for Current Status and Perspectives. *Resour., Conserv. Recycl.* **2020**, No. 104787, DOI: 10.1016/j.resconrec.2020.104787.
(30) Xu, B.; Chen, Y.; Zhou, Y.; Zhang, B.; Liu, G.; Li, Q.; Yang, Y.; Jiang, T. A Review of Recovery of Palladium from the Spent Automobile Catalysts. *Metals* **2022**, 533 DOI: 10.3390/met12040533.
(31) Ahtiainen, R.; Lundström, M. Cyanide-Free Gold Leaching in Exceptionally Mild Chloride Solutions. *J. Clean Prod* **2019**, *234*, 9−17.
(32) Li, X. guang; Gao, Q.; Jiang, S. qi; Nie, C. chen; Zhu, X. nan; Jiao, T. tian Review on the Gentle Hydrometallurgical Treatment of WPCBs: Sustainable and Selective Gradient Process for Multiple Valuable Metals Recovery. *J. Environ. Manage.* **2023**, No. 119288, DOI: 10.1016/j.jenvman.2023.119288.
(33) Méndez, A.; Nogueira, C. A.; Paiva, A. P. Recovery of Platinum from a Spent Automotive Catalyst through Chloride Leaching and Solvent Extraction. *Recycling* **2021**, *6* (2), 27.
(34) Altansukh, B.; Haga, K.; Huang, H. H.; Shibayama, A. Gold Recovery from Waste Printed Circuit Boards by Advanced Hydrometallurgical Processing. *Mater. Trans* **2019**, *60* (2), 287−296.
(35) Krishnan, S.; Zulkapli, N. S.; Kamyab, H.; Taib, S. M.; Din, M. F. B. M.; Majid, Z. A.; Chaiprapat, S.; Kenzo, I.; Ichikawa, Y.; Nasrullah, M.; Chelliapan, S.; Othman, N. Current Technologies for Recovery of Metals from Industrial Wastes: An Overview. *Environ. Technol. Innovation* **2021**, No. 101525, DOI: 10.1016/j.eti.2021.101525.
(36) Ji, X.; Shen, Z.; Xu, W.; Yao, S.; Zhang, H.; Xiong, L.; Li, H.; Guo, H.; Chen, X.; Chen, X. Current Progress on Gold Recovery from Refractory Ore and Waste Electrical and Electronic Equipment. *Kor. J. Chem. Eng.* **2023**, 2046−2059, DOI: 10.1007/s11814-023-1449-4.
(37) Rzelewska-Piekut, M.; Paukszta, D.; Regel-Rosocka, M. Hydrometallurgical Recovery of Platinum Group Metals from Spent Automotive Converters. *Physicochemical Problems of Mineral Processing* **2021**, *57* (2), 83−94.
(38) Marra, A.; Cesaro, A.; Belgiorno, V. Recovery Opportunities of Valuable and Critical Elements from WEEE Treatment Residues by Hydrometallurgical Processes. *Environmental Science and Pollution Research* **2019**, *26* (19), 19897−19905.
(39) Minoda, A.; Miyashita, S. I.; Kondo, T.; Ogura, T.; Sun, J.; Takahashi, Y. Low-Concentration Palladium Recovery from Diluted Aqua Regia-Based Wastewater Using Lyophilized Algal Cells. *Resources, Conservation and Recycling Advances* **2023**, *17*, No. 200140.
(40) Nguyen, V. T.; Riaño, S.; Aktan, E.; Deferm, C.; Fransaer, J.; Binnemans, K. Solvometallurgical Recovery of Platinum Group Metals from Spent Automotive Catalysts. *ACS Sustain Chem. Eng.* **2021**, *9* (1), 337−350.
(41) Chang, Z.; Zeng, L.; Sun, C.; Zhao, P.; Wang, J.; Zhang, L.; Zhu, Y.; Qj, X. Adsorptive Recovery of Precious Metals from Aqueous Solution Using Nanomaterials − A Critical Review. *Coord. Chem. Rev.* **2021**, No. 214072, DOI: 10.1016/j.ccr.2021.214072.
(42) Trucillo, P.; Lancia, A.; Di Natale, F. Recovery of Platinum from Diesel Catalysts by Combined Use of H2O2/HCl Leaching and Adsorption. *J. Environ. Chem. Eng.* **2022**, *10* (3), No. 107730.
(43) Trucillo, P.; Di Maio, E.; Lancia, A.; Di Natale, F. Selective Gold and Palladium Adsorption from Standard Aqueous Solutions. *Processes* **2021**, *9* (8), 1282.
(44) Di Natale, F.; Orefice, M.; La Motta, F.; Erto, A.; Lancia, A. Unveiling the Potentialities of Activated Carbon in Recovering Palladium from Model Leaching Solutions. *Sep Purif Technol.* **2017**, *174*, 183−193.
(45) Cheng, N.; Zhang, L.; Wang, M.; Shu, J.; Shao, P.; Yang, L.; Meng, X.; Fan, Y.; Li, M. Highly Effective Recovery of Palladium from a Spent Catalyst by an Acid- and Oxidation-Resistant Electrospun Fibers as a Sorbent. *Chem. Eng. J.* **2023**, *466*, No. 143171.
(46) Zhao, H.; Chi, H. Electrospun Bead-on-String Fibers: Useless or Something of Value? *Novel Aspects Nanofibers* **2018**, 87 DOI: 10.5772/intechopen.74661.
(47) Chen, W.; Zhao, P.; Yang, Y.; Yu, D. Electrospun Beads-on-the-String Nanoproducts: Preparation and Drug Delivery Application. *Curr. Drug Delivery* **2023**, *20*, 1224 DOI: 10.2174/1567201819666220525095844.
(48) Chrysafi, I.; Avraam, K.; Krasia-Christoforou, T. Bead-Free and Beaded Electrospun Phase Change Fibers: A Comparative Study. *Eur. Polym. J.* **2023**, *191*, No. 112037.
(49) Shenoy, S. L.; Bates, W. D.; Frisch, H. L.; Wnek, G. E. Role of Chain Entanglements on Fiber Formation during Electrospinning of

Polymer Solutions: Good Solvent, Non-Specific Polymer-Polymer Interaction Limit. *Polymer (Guildf)* **2005**, *46* (10), 3372−3384.
(50) Munir, M. M.; Suryamas, A. B.; Iskandar, F.; Okuyama, K. Scaling Law on Particle-to-Fiber Formation during Electrospinning. *Polymer (Guildf)* **2009**, *50* (20), 4935−4943.
(51) Aziz, S. B.; Marif, R. B.; Brza, M. A.; Hassan, A. N.; Ahmad, H. A.; Faidhalla, Y. A.; Kadir, M. F. Z. Structural, Thermal, Morphological and Optical Properties of PEO Filled with Biosynthesized Ag Nanoparticles: New Insights to Band Gap Study. *Results Phys.* **2019**, *13*, No. 102220.
(52) Pucić, I.; Jurkin, T. FTIR Assessment of Poly(Ethylene Oxide) Irradiated in Solid State, Melt and Aqeuous Solution. *Radiat. Phys. Chem.* **2012**, *81* (9), 1426−1429.
(53) Ramesh, S.; Leen, K. H.; Kumutha, K.; Arof, A. K. FTIR Studies of PVC/PMMA Blend Based Polymer Electrolytes. *Spectrochim Acta A Mol. Biomol Spectrosc* **2007**, *66* (4−5), 1237−1242.
(54) Gu, D.; Zhang, L.; Chen, S.; Song, K.; Liu, S. Significant Reduction of the Friction and Wear of PMMA Based Composite by Filling with PTFE. *Polymers (Basel)* **2018**, *10* (9), 966.
(55) Geng, Y.; Li, J.; Lu, W.; Wang, N.; Xiang, Z.; Yang, Y. Au(III), Pd(II) and Pt(IV) Adsorption on Amino-Functionalized Magnetic Sorbents: Behaviors and Cycling Separation Routines. *Chem. Eng. J.* **2020**, *381*, No. 122627.
(56) Lin, S.; Zhao, Y.; Bediako, J. K.; Cho, C. W.; Sarkar, A. K.; Lim, C. R.; Yun, Y. S. Structure-Controlled Recovery of Palladium(II) from Acidic Aqueous Solution Using Metal-Organic Frameworks of MOF-802, UiO-66 and MOF-808. *Chemical Engineering Journal* **2019**, *362*, 280−286.
(57) da Silva, T. L.; da Silva, M. G. C.; Vieira, M. G. A. Palladium Adsorption on Natural Polymeric Sericin-Alginate Particles Cross-linked by Polyethylene Glycol Diglycidyl Ether. *J. Environ. Chem. Eng.* **2021**, *9* (4), No. 105617.
(58) Wojnicki, M.; Socha, R. P.; Pędzich, Z.; Mech, K.; Tokarski, T.; Fitzner, K. Palladium(II) Chloride Complex Ion Recovery from Aqueous Solutions Using Adsorption on Activated Carbon. *J. Chem. Eng. Data* **2018**, *63* (3), 702−711.
(59) Sato, T.; Abe, S.; Ito, S.; Abe, T. Silk Fibroin Fiber for Selective Palladium Adsorption: Kinetic, Isothermal and Thermodynamic Properties. *J. Environ. Chem. Eng.* **2019**, *7* (2), No. 102958.
(60) Godlewska-Zyłkiewicz, B.; Sawicka, S.; Karpińska, J. Removal of Platinum and Palladium from Wastewater by Means of Biosorption on Fungi Aspergillus Sp. and Yeast Saccharomyces Sp. *Water* **2019**, *11* (7), 1522.
(61) Grad, O.; Ciopec, M.; Negrea, A.; Duţeanu, N.; Vlase, G.; Negrea, P.; Dumitrescu, C.; Vlase, T.; Vodă, R. Precious Metals Recovery from Aqueous Solutions Using a New Adsorbent Material. *Sci. Rep.* **2021**, *11* (1), 2016 DOI: 10.1038/s41598-021-81680-z.
(62) Nagireddi, S.; Golder, A. K.; Uppaluri, R. Role of Protonation and Functional Groups in Pd(II) Recovery and Reuse Characteristics of Commercial Anion Exchange Resin-Synthetic Electroless Plating Solution Systems. *Journal of Water Process Engineering* **2018**, *22*, 227−238.
(63) Di Natale, F.; Gargiulo, V.; Alfè, M. Adsorption of Heavy Metals on Silica-Supported Hydrophilic Carbonaceous Nanoparticles (SHNPs). *J. Hazard Mater.* **2020**, *393*, No. 122374.
(64) Di Natale, F.; Erto, A.; Lancia, A.; Musmarra, D. Equilibrium and Dynamic Study on Hexavalent Chromium Adsorption onto Activated Carbon. *J. Hazard Mater.* **2015**, *281*, 47−55.

https://doi.org/10.1021/acsapm.4c00324
ACS Appl. Polym. Mater. 2024, 6, 9406−9419